energies

MDPI

Article

Approaching the Theoretical Maximum Performance of Highly Transparent Thermochromic Windows

Daniel Mann [1,2,*], Lavinia Calvi [3,4,5], Cindy P. K. Yeung [1,2], Roberto Habets [1,2], Ken Elen [3,4,5], An Hardy [3,4,5], Marlies K. Van Bael [3,4,5] and Pascal Buskens [1,2,3,*]

1 The Netherlands Organisation for Applied Scientific Research (TNO), High Tech Campus 25, 5656 AE Eindhoven, The Netherlands
2 Brightlands Materials Center, Urmonderbaan 22, 6167 RD Geleen, The Netherlands
3 Design and Synthesis of Inorganic Materials (DESINe), Institute for Materials Research, Hasselt University, Agoralaan Building D, 3590 Diepenbeek, Belgium
4 IMEC vzw, IMOMEC Associated Laboratory, Wetenschapspark 1, 3590 Diepenbeek, Belgium
5 EnergyVille, Thor Park 8320, 3600 Genk, Belgium
* Correspondence: daniel.mann@tno.nl (D.M.); pascal.buskens@tno.nl (P.B.)

Abstract: Thermochromic window coatings represent a promising technology to improve the energy efficiency of buildings in intermediate climates. With the technology approaching market introduction it is important to investigate its performance limits within smart windows and to identify existing development challenges. Here we analyze the theoretical maximum performance of thermochromic window coatings that modulate IR transmission whilst retaining high visible transparency. The set limitations lead to a theoretical maximum solar modulation of 39.1%. Within an insulated glazing unit (IGU), where at least 2 glass panes and a conventional low-e coating are required, this value is further reduced to 12.9%. We show that by carefully selecting a low-e coating with the highest compatibility to a thermochromic coated glass and by allowing 10% of modulation in the visible spectral range, the theoretical maximum can be increased to 23.1%, illustrating the importance to codesign and match both coatings within a smart window to reach optimum performance. Furthermore, we compared our current best-performing VO_2:SiO_2 composite coating within an IGU to the theoretical maximum. The analysis shows that with a solar modulation of 13.4%, the coating is currently at 59% of the theoretical maximum. Finally, we propose and discuss several strategies to proceed further toward the theoretical maximum.

Keywords: smart window; solar modulation; simulation; thermochromic; vanadium dioxide; energy efficiency

Citation: Mann, D.; Calvi, L.; Yeung, C.P.K.; Habets, R.; Elen, K.; Hardy, A.; Van Bael, M.K.; Buskens, P. Approaching the Theoretical Maximum Performance of Highly Transparent Thermochromic Windows. *Energies* **2023**, *16*, 4984. https://doi.org/10.3390/en16134984

Academic Editors: Ricardo M. S. F. Almeida and Eva Barreira

Received: 23 May 2023
Revised: 21 June 2023
Accepted: 22 June 2023
Published: 27 June 2023

1. Introduction

In the process of increasing the energy efficiency of buildings, most building components require optimization to minimize interaction with the outside environment. Buildings are made air-tight, and the insulation of walls, roofs, and floors is further increased to realize a static indoor climate [1]. The part of the building skin for which interaction with the outside is still desired, are windows. For windows, capturing natural light and solar heat is desired to a certain extent. It has been demonstrated that sunlight and solar heat have a positive influence on people's health and well-being [2] and all solar energy that can be directly used in a building for lighting and heating reduces the overall energy costs [3]. However, when certain irradiance levels are surpassed, glare becomes an issue, and shading is desired. In addition, solar heat transmission through windows accounts for 60% of the total solar heat gain in buildings. As a result, overheating of buildings and air-conditioning demand to reduce indoor temperatures are largely based on solar transmission through windows [4]. Therefore, the requirements for visible (T_{vis}) and total solar (T_{sol}) transmission vary depending on the climate zone and the amount of window surface [3,5]. The glass

industry is approaching these different demands by offering static glazing with different T_{vis} and g values (the g value equals the total solar energy transmitted through a window, radiative and conductive) [6]. A wide range of different products are available which have been optimized over the past decades. However, since in many climate regions a building's demands on sunlight and solar heat transmission change during the day and between the seasons, static glazing can never capture the full potential of sunlight.

Traditionally, the inability of windows to adapt to the changing requirement for sunlight and solar heat transmission has been accommodated by using external or internal shading devices [7]. Since all these shading devices themselves have certain limitations, like not being able to distinguish between visible light and solar heat transmission, recent development has been focused on smart windows that can adapt their interaction with sunlight directly upon an external stimulus [8]. Electrochromic windows are the most advanced of all smart window technologies, with several products already available on the market [9,10]. Due to their complexity and the necessity for wiring and special frames, these technologies are expensive and therefore still limited to niche applications. Since the costs cannot be earned back via energy savings in a reasonable amount of time, electrochromic smart windows are focused on increasing comfort via actively adjusting the shading of the glass and therefore providing privacy, as well as reducing glare and solar heat gain [11]. Another smart window technology that is being developed is photochromic windows. Photochromic glazing technology is already commercially applied in sunglasses that increase shading at high solar irradiance levels. In the same way, photochromic windows can be used to increase shading and reduce glare [8]. As already inherent to the technology, photochromic materials are foremost applicable for glare control. It is difficult to optimize photochromic windows for minimum energy demand, due to the fact that irradiance levels are not the best trigger to determine when to transmit or block solar heat. For example, on sunny winter days, the high irradiance levels can induce tinting, although low ambient temperatures make solar heat gain still beneficial for the energy demand. Thermochromic materials are best suited to be optimized for energy efficiency alone [12,13]. They can be designed to minimize the impact on T_{vis}, whilst modulating infrared (IR) transmission and therefore solar heat gain. Temperature as the external trigger is best suited to couple with a building's thermostat by adjusting the transition temperature in the thermochromic material. Additionally, the material does not require special equipment to trigger the switch and can be installed like regular windows. This way, thermochromic windows can be designed for use in regular insulated glazing units (IGUs) enabling optimum use of solar heat whilst retaining high visible transparency.

Because of their high application potential, thermochromic materials—mainly vanadium dioxide (VO_2)—have been a research focus in the last years [12–14]. Materials for thermochromic smart windows have been optimized by increasing solar modulation (ΔT_{sol}) values at high T_{vis} [15–18]. Switching temperatures have been optimized to cover a wide range between 0 and 68 °C [19,20], increasing the potential to tune the properties to requirements in various climate zones. Furthermore, processes are being scaled up and production costs are being reduced [17,21]. The potential of thermochromic smart windows has been analyzed in several simulation studies [22], including the impact of switching temperature and hysteresis [23], and it has been shown that these new technologies surpass commercial glazing in energy efficiency in intermediate climates [3]. Nevertheless, most of the studies optimizing the performance of thermochromic windows, as well as many simulation studies, are studying the optical properties of the thermochromic material isolated from the real application in smart windows. But windows are not only important for their solar heat gain, but they are also the most vulnerable part of the building skin with respect to radiator heat loss. To increase the insulation value of windows, the number and thickness of glass panes as well as the number, width and atmosphere of gas spaces between the glass panes can be adjusted. In addition, the glass panes can be coated with a low emissivity (low-e) coating, significantly reducing the thermal conductivity of an IGU [24]. Since these low-e coatings not only impact infrared radiation between 5–25 µm, and therefore the

emissivity, but also near-IR transmission, they have to be accounted for when analyzing the impact of thermochromic glazing. To realize insulation values (u values) of thermochromic smart windows in agreement with current standards, a combination of thermochromic glass and low-e coated glass is required. We have shown in a recent simulation study that only with such a combination the positive effect of changing solar heat gain can be realized. However, the low-e coating properties of partly blocking solar near-IR light reduces the solar modulation of the complete IGU [3]. This shows the necessity of codesigning all components of the IGU and investigating a perfect combination of thermochromic and low-e properties.

Since thermochromic smart windows are approaching market introduction, it is important to investigate the performance limit of smart windows, to identify existing development challenges [25]. For that purpose, we study practical combinations of our thermochromic glass with best-in-class optical performance (combination of visible transmission and solar modulation) [15] with selected commercially available low-e glasses. Here we report a detailed study on the maximum theoretical solar modulation when focusing solely on the IR part of the solar spectrum. Furthermore, we investigate how the theoretical maximum changes when applied in an IGU with different low-e coatings, and when including 10% of visible transmission in the modulated range. Additionally, we compare one of our high-performance thermochromic smart window coatings to these theoretical maximum values to investigate which major challenges are to overcome, and we give an outlook on how to optimize these coatings to come closer to their theoretical maximum performance.

2. Methods

2.1. Theoretical Investigation

For investigation of potential transmission modulation via thermochromic smart windows for several combinations of different glazing options, the UV-vis-NIR transmission spectrum of a commercial glass or combination of two glasses in an IGU was compared to a manipulated version of the respective spectrum, where transmission was set to 0 in wavelength regions > 780 nm. The two spectra were compared by calculating the total solar transmission (T_{sol}) and the solar modulation (ΔT_{sol}). T_{vis}, T_{sol} and ΔT_{sol} were calculated using the following formulas:

$$T_{vis,sol} = \frac{\int \phi_{vis,sol}(\lambda) T(\lambda) d\lambda}{\int \phi_{vis,sol}(\lambda) d\lambda} \quad (1)$$

$$\Delta T_{sol} = T_{sol,cold} - T_{sol,hot} \quad (2)$$

with $T(\lambda)$ as the transmittance at wavelength λ, $\Phi_{vis}(\lambda)$ as the photopic spectral sensitivity of human vision, and $\Phi_{sol}(\lambda)$ as the AM 1.5 solar irradiance spectrum. For IGUs also modulations of g values (Δg) were calculated. Here g values were calculated according to EN410 [26]. For each IGU the following assumptions were made (Figure S1): (i) double glazing with 2 glass panes and 1 gas space; (ii) glass thickness 4 mm; (iii) gas space 12 mm; (iv) gas space atmosphere argon; (v) adaptive glass as outer glass pane with coating on surface 2; (vi) coating of inner glass pane on surface 3.

The following glasses and glazing systems have been used in the study (Table 1).

Table 1. Glasses and glazing systems used in this study.

Glass				Glazing System (Outer Glass Pane × Inner Glass Pane)
Product Name	**Manufacturer**	**Type of Glass**	**Thickness**	
Optifloat Clear	Pilkington, Lathom, UK	Monolithic	4 mm	
ECLAZ	Saint-Gobain, Courbevoie, France	Coated	4 mm	Optifloat × ECLAZ
Isolide Superplus	Scheuten Glas, Venlo, The Netherlands	Coated	4 mm	Optifloat × Isolide
SunCool 70/40Pro	Pilkington, Lathom, UK	Coated	6 mm *	Optifloat × SunCool
SunSmart 67/23	TNO, Geleen, The Netherlands	Coated/thermochromic	4 mm	SunSmart × ECLAZ

* The SunCool series was only available in 6 and 12 mm thickness in the database. However the deviation in glass thickness is not expected to have a major impact on the conducted analysis.

Optical properties of coated (Scheuten Isolide and TNO SunSmart) and uncoated (Pilkington Optifloat) glass plates have been measured via UV-vis-NIR spectrophotometry using a Perkin Elmer Lambda 750 (Perkin Elmer, Inc., Waltham, MA, USA) with integrating sphere and a customized module comprising a heating element equipped with a module for measuring transmission and reflection in the wavelength regions between 300 nm and 2400 nm. Optical data of commercial low-e coated glass (Saint-Gobain ECLAZ and Pilkington SunCool) have been used from the International Glazing Database (IGDB) within the WINDOW program (version 7.6) by Berkeley Labs [27]. The transmission spectra of all glasses used in this study are presented in Figure 1. T_{vis} and T_{sol} of glazing systems have been calculated using the Optics program by Berkeley Labs [27] and transmission spectra have been calculated using the following formula:

$$T_{glazing\ system}(\lambda) = T_{glass\ pane\ 1}(\lambda) \times T_{glass\ pane\ 2}(\lambda) \quad (3)$$

with $T(\lambda)$ as the transmittance at wavelength λ.

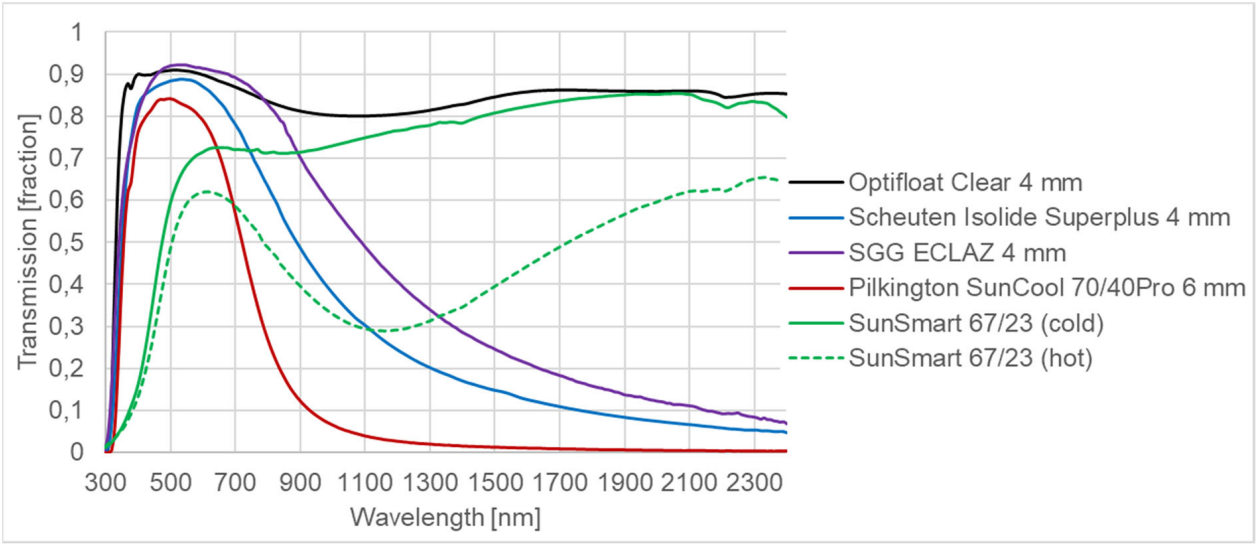

Figure 1. UV-vis-NIR transmission spectra of coated and uncoated glass plates used in this study.

2.2. Coating Preparation

The thermochromic coating used in this study was prepared in analogy to a previously published procedure [15]. One side of a barrier coated glass substrate was masked using d-c-fix® self-adhesive foil. Subsequently, the thermochromic coating was applied to the non-covered, tin side using dip coating. The applied liquid coating formulation consisted of a mixture of vanadyl oxalate solution and silica at a SiO_2 to VO_2 ratio of 2.2:1 w/w. The xerogel coating was applied to the glass substrates at a withdrawal speed in the range

of 8.0 mm·s^{-1} to achieve the desired thickness. After drying for 5 min under ambient conditions, the adhesive foil was removed. The non-coated side was then placed onto a 6 inch silica wafer, and annealed in a Jipelec Jetfirst PV Rapid Thermal Processor (ECM, Grenoble, France), with the coated side facing the IR radiators. The coated glass plates were first heated to 270 °C in air for 480 s, and subsequently in N_2 at 450 °C for 30 s.

3. Results and Discussion

3.1. Investigation of Theoretical Maximum Performance

To investigate the theoretical maximum solar modulation for adaptive glazing, we started by analyzing the wavelength dependent light transmission of clear glass. Here we measured the UV-vis-NIR transmission of a 4 mm Pilkington Optifloat Clear glass and calculated the solar properties. The wavelength dependent transmission spectrum can be seen in Figure 1. The glass plate showed a T_{vis} of 90.3% and a T_{sol} of 85.4% (Table 2). According to EN 410 [22], visible transmission is defined as the region between 380–780 nm. Therefore, if the solar modulation should be limited to the IR region, all light transmitted >780 nm could theoretically be blocked. To simulate this theoretical blocking state, the light transmission between 780–2500 nm was set to 0, whilst retaining the wavelength dependent transmission between 300–780 nm of the Optifloat Clear glass. The thereby obtained theoretical transmission spectrum of a total IR blocking state (blocking >780 nm) was used to calculate the theoretical solar properties. Since T_{vis} was not influenced by the data manipulation, the same value as for the Optifloat Clear glass was obtained, whereas the T_{sol} value dropped to 46.3% (Table 2). Directly comparing the transmission spectrum of Optifloat Clear glass with the theoretical IR blocking state shows that a large part of the transmission can be modulated even by solely focusing on the IR (Figure 2). Since solar intensity drops significantly in higher wavelength regions and the IR only accounts for approximately 45% of the total solar radiation, the maximum theoretical solar modulation ΔT_{sol} between these two states is 39.1% (Table 2).

Table 2. Solar properties of measured and theoretical glass and glazing systems with potential solar modulation for various scenarios.

Glass/Glazing System	Scenario	T_{vis} [%]	T_{sol} [%]	ΔT_{sol} [%]
Optifloat Clear	Full transmission	90.3	85.4	39.1
	blocking > 780 nm	90.3	46.3	
Optifloat × ECLAZ	Full transmission	83.2	60.3	19.0
	blocking > 780 nm	83.2	41.3	
	blocking > 780 + 10% vis	74.9	37.2	23.1
Optifloat × Isolide	Full transmission	79.8	51.3	12.9
	blocking > 780 nm	79.8	38.4	
Optifloat × SunCool	Full transmission	73.7	35.8	3.1
	blocking > 780 nm	73.7	32.7	
SunSmart	Cold state	67.1	67.7	22.9
	Hot state	57.4	44.8	
SunSmart × ECLAZ	Cold state	61.7	45.7	13.4
	Hot state	52.8	32.3	

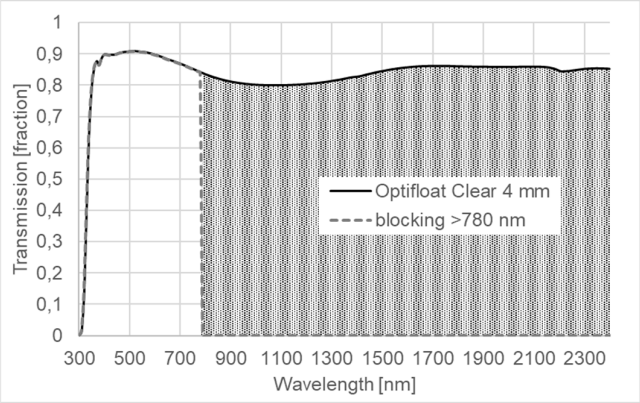

Figure 2. UV-vis-NIR transmission spectrum of Optifloat Clear glass (full line) and theoretical spectrum with 0% transmission > 780 nm (dotted line) with potential modulation range marked as dotted.

The analyzed optical properties of Optifloat Clear glass and the potential solar modulation of 39.1% for an adaptive glazing would be representative of single glazing. But this type of glazing has a very low insulation value of 5.8 W/m^2 K and therefore leads to significant radiator heat loss. Current standard glazing for newly built homes in the Netherlands is so-called HR++ glazing with an insulation value of 1.1 W/m^2 K, with similar standards for windows in most European countries. These are insulated glazing units (IGUs) made of 2 glass panes of which one is coated with a low-e coating and a gas space commonly filled with a low thermal conductivity gas, such as argon. This type of glazing has different optical properties from a single Optifloat Clear glass, especially in the IR. Therefore, to assess the theoretical maximum solar modulation of an adaptive glazing within a current state-of-the-art IGU, we investigated the optical properties of an IGU combining an Optifloat Clear glass with a Scheuten Isolide Superplus glass. In the UV-vis-NIR transmission spectrum, it can be seen that the Isolide Superplus glass still shows a high visible transmission, but the transmission in the IR drops significantly, especially in longer wavelength regions (Figure 1). In the IGU the transmission over the whole wavelength region drops slightly due to the transmission of the Optifloat glass between 80–90% for all wavelengths between 350–2500 nm (Figure 3). Overall, the representative HR++ glazing shows solar properties of T_{vis} = 79.8% and T_{sol} = 51.3% (Table 2). This means that the combination Optifloat x Isolide already blocks 48.7% of solar radiation from entering the building, which significantly reduces the amount of sunlight that can be modulated. To investigate the amount of IR light that can still be modulated within such an IGU, we simulated a theoretical IR blocking state with 0% IR transmission. To calculate the optical properties of such a glazing system, we combined the Isolide glass with the theoretical blocking > 780 nm glass. Such a combination showed again unchanged T_{vis} of 79.8% and a reduced T_{sol} of 38.4%. Comparing the UV-vis-NIR transmission spectrum of the Optifloat × Isolide combination with the theoretical blocking > 780 nm × Isolide state, it can be seen that the amount of IR light that can be modulated is reduced significantly in comparison to the Optifloat single glass (Figures 2 and 3). Overall the theoretical maximum ΔT_{sol} drops to 12.9% for the HR++ glass.

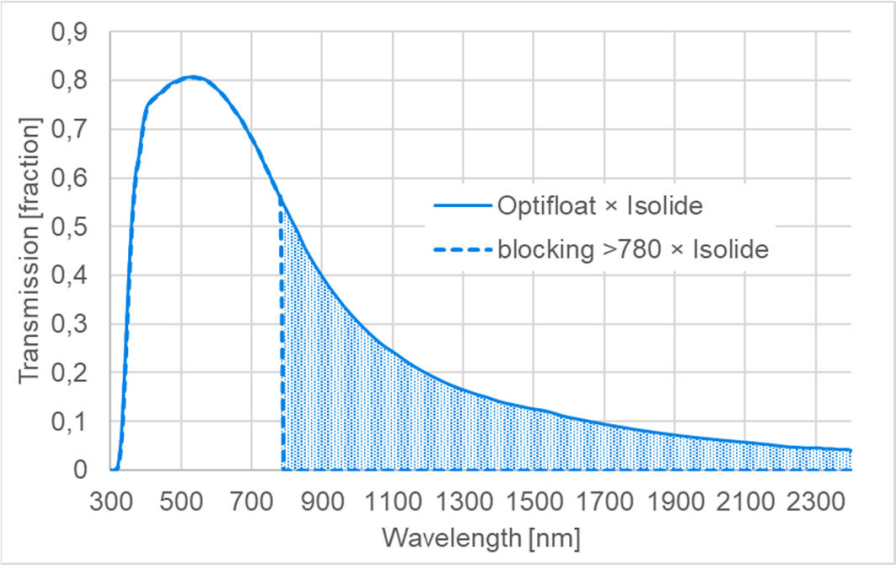

Figure 3. UV-vis-NIR transmission spectrum of Optifloat × Isolide glazing system (full line) and theoretical blocking > 780 nm × Isolide state with 0% IR transmission (dotted line) with potential modulation range marked as dotted.

Even though the Scheuten Isolide is a representative of the most common low-e coated glasses used in IGUs for residential buildings, there are other low-e coatings on the market that block more or less IR light. Since adaptive glazing can in general be combined with any low-e coated glass to reach an insulation value of 1.1 W/m^2 K, it is important to select the best suited low-e coated glass. The suitability here can be equated to the maximum possible solar modulation. To investigate the theoretical maximum solar modulation of IGUs with different low-e coated glasses and their suitability to be used in adaptive glazing systems, we calculated the solar properties of 2 additional IGUs with a highly transparent low-e coating and a so-called solar control coating, that blocks a large part of IR light. As highly transparent low-e coating we selected the Saint-Gobain ECLAZ series. Combined with an Optifloat clear glass in an IGU, a T_{vis} of 83.2% and T_{sol} of 60.3% were obtained (Table 2). The solar control glazing, where we selected Pilkington's SunCool series as a representative case study, resulted in T_{vis} values of 73.7% and T_{sol} of 35.8% (Table 2). Here it could already be observed that the solar control coating blocks a large part of IR light and therefore leaves little room for modulation via adaptive glazing (Figure 1). To calculate ΔT_{sol} values and to compare the different low-e coatings, we again calculated transmission spectra where we combined the individual low-e coated glasses with the theoretical blocking > 780 nm spectrum. By comparing the IGUs with different low-e coatings with each other as well as with the respective theoretical IR blocking states, it was observed that the combination Optifloat × ECLAZ has the highest potential modulation range in the IR (Figure 4). Here, for the blocking state, a T_{sol} of 41.3% was calculated, which results in a ΔT_{sol} of 19.0% (Table 2). For the solar control glazing the blocking state had a T_{sol} of 32.7% which is not much lower than for the regular combination Optifloat × SunCool and therefore leads only to a ΔT_{sol} of 3.1%. The potential solar modulation of the HR++ glazing lies at 12.9% between those two. Since the highly transparent low-e coating (Saint-Gobain ECLAZ) transmits the largest part of IR light for all 3 studied low-e coatings it has the highest potential and best suitability to be combined with adaptive glazing.

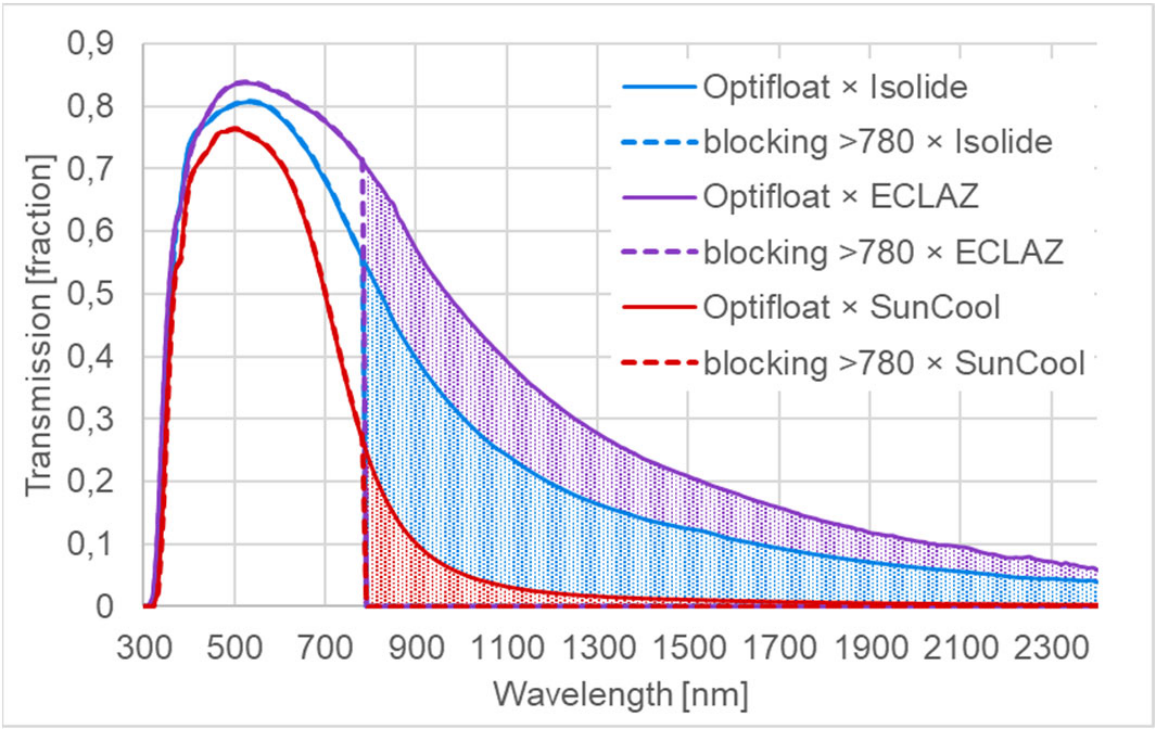

Figure 4. UV-vis-NIR transmission spectra of glazing systems with different low-e coated glasses (full line) and all whilst theoretically blocking all light > 780 nm (dotted line) with potential modulation range marked as dotted.

Even though VO_2 based thermochromic coatings are aimed at staying highly transparent in the visible and solely modulating the IR region of sunlight, especially high-performing nanocomposite coatings [15] or coatings within anti-reflective coating stacks [28] also show a slight modulation in the visible range. Here, it has been shown that adding modulation of a few percent in the visible to a large modulation in the IR can significantly increase the overall ΔT_{sol} of a thermochromic coating. Furthermore, if the change in visible transmission is kept at a few percent, the change is barely visible to the human eye and the coated glass still appears highly transparent. To investigate the potential solar modulation of an IGU with an ECLAZ low-e coated glass, where full IR modulation is combined with partial modulation of visible light, we simulated a second theoretical blocking transmission spectrum. In accordance with the blocking > 780 nm spectrum, we started from the Optifloat Clear transmission spectrum whilst setting transmission > 780 nm to 0. In addition, we reduced the transmission of the Optifloat transmission spectrum $\leq$ 780 nm by 10%. This theoretical blocking > 780 + 10% vis spectrum was combined with the ECLAZ spectrum to simulate a theoretical blocking state of the IGU (Figure 5). For this blocking state, a T_{vis} of 74.9% and T_{sol} of 37.2% were calculated (Table 2). Comparing this with the transmission of the Optifloat × ECLAZ IGU, it can be seen that T_{vis} is reduced by 8.3% and a ΔT_{sol} of 23.1% is obtained. Since a larger modulation in the visible is not desired and the ECLAZ low-e coating shows the highest potential for solar modulation, it can be concluded that within these limitations a ΔT_{sol} of 23.1% is the theoretical maximum that can be achieved with VO_2 based thermochromic coatings within an IGU.

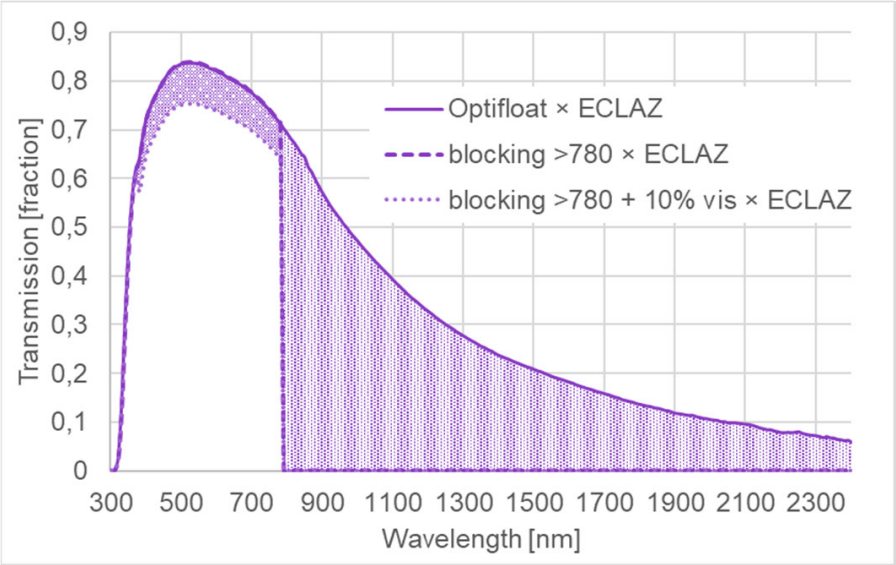

Figure 5. UV-vis-NIR transmission spectrum of Optifloat × ECLAZ glazing system (full line), theoretical blocking > 780 nm × ECLAZ state with 0% IR transmission (dotted line) and additional blocking in the visible (blocking > 780 + 10% vis; small dotted line) with potential modulation ranges marked as dotted.

3.2. Current Record Performance

After assessing in detail the theoretical maximum solar modulation of a VO_2 based thermochromic coating within an IGU, we compared the properties of our current best-performing coating to these values. The coating we selected is a VO_2:SiO_2 composite coating, where the composition and coating thickness is optimized to realize an optimum combination of high T_{vis} of 67.1% and large ΔT_{sol} of 22.9%. A high T_{vis} is obtained via the integration of VO_2 domains in an SiO_2 matrix, which increases transparency and simultaneously reduces reflection via a reduced refractive index of the composite layer. In addition, the composition is optimized to create small evenly distributed VO_2 domains with an average size < 30 nm, which leads to increased light absorption in the rutile state (hot state) in wavelength regions between 800–1300 nm. This effect for small VO_2 domains within a coating matrix has been attributed in literature to an occurring plasmonic absorption of the metallic VO_2 phase [29,30]. The increased absorption in this wavelength region has a big impact on the overall T_{sol} in the hot state, since the solar IR intensity is highest between 780–1360 nm (Figure S2). Since solar IR intensity decreases >1400 nm significantly, the higher transmission of our SunSmart coating in the hot state in these wavelength regions does not negatively impact the overall ΔT_{sol}. By carefully designing the transmission of the thermochromic coating in both cold and hot states, the large ΔT_{sol} of 22.9% can be reached. To investigate the optical properties of a Smart Window IGU, we calculated the transmission spectra by combining our thermochromic coated glass with an ECLAZ low-e coated glass (Figure 6). For the cold state, we obtained T_{vis} values of 61.7% and T_{sol} of 45.7%, whereas for the hot state, we obtained a reduced T_{vis} of 52.8% and T_{sol} of 32.3% (Table 2). Overall we obtained a reduction in T_{vis} of 8.9%, which is similar to the blocking > 780 +10% vis × ECLAZ combination, and a ΔT_{sol} of 13.4%. A significant reduction in ΔT_{sol} in comparison to the single thermochromic coated glass can be observed, which is due to the IR-blocking properties of the ECLAZ coating. However, here also the designed optical properties with an increased modulation in the region between 800–1300 nm are beneficial, since in this region the ECLAZ coating still has a relatively high transparency, whereas >1400 nm the transparency drops significantly. Comparing the performance of the SunSmart IGU with the theoretical maximum performance, it can be concluded that the ΔT_{sol} of 13.4% is at 59% of the theoretical maximum.

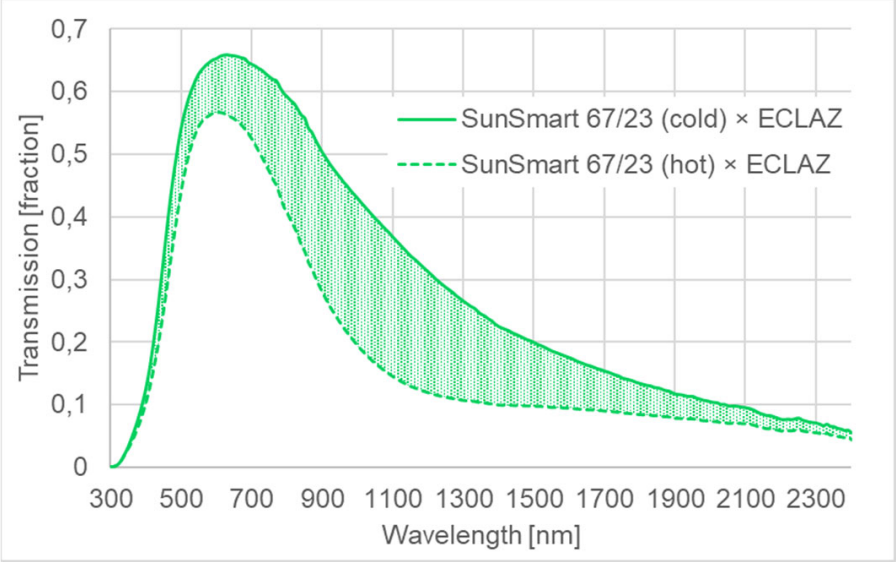

Figure 6. UV-vis-NIR transmission spectrum of SunSmart × ECLAZ glazing system in the cold (full line) and hot state (dotted line) with modulation range marked as dotted.

3.3. Optimization Strategies to Approach Theoretical Maximum

With 59% of theoretical maximum performance, the current SunSmart coating already shows very good properties. However, optimization of the coating and the active material can further improve the performance to bring the resulting solar modulation closer to its theoretical maximum. By careful analysis of the composite coating, as well as optimization strategies in literature, we have identified four strategies to further optimize the solar modulation that will be elaborated in more detail.

3.3.1. Purity of Active Material

VO_2 can exist in an amorphous, as well as in various crystalline phases, of which only the monoclinic phase shows thermochromic properties [31]. Furthermore, vanadium can exist in several oxidation states ranging from +2 up to +5 [32]. Therefore, VO_2 in the oxidation state +4, can be easily oxidized or reduced. Since all vanadium species show distinct absorption in the visible, but only VO_2(M) has thermochromic properties, the T_{vis} of a coating is impacted by the total vanadium content, whereas ΔT_{sol} is only impacted by the VO_2(M) content. Therefore, to optimize the combination of high T_{vis} with high ΔT_{sol} it is important to increase the share of active VO_2(M) in the total vanadium content of a thermochromic coating.

In an earlier study, we investigated the purity of VO_2(M) in a VO_2:SiO_2 composite coating made from liquid precursors [15]. Here we could show that only 54% of the total vanadium content was crystalline VO_2(M). Since no other crystal phases or oxidation states were found, the remaining content was most probably amorphous VO_2. Therefore, further improving the purity of the VO_2(M) content via careful adjustment of the coating formulation and thermal anneal process can further improve the thermochromic performance.

Another possibility to produce thermochromic VO_2 coatings is by synthesizing VO_2 pigments and integrating those in a coating matrix. Here the purity of the VO_2(M) content can be more easily controlled, since the crystallization of VO_2(M) is decoupled from the coating formation. However, also the synthesis of VO_2 nanoparticles brings many challenges to achieving phase pure monoclinic material with a high switching enthalpy. Additionally, doping, which is required to reduce the switching temperature to application-oriented values, may also lead to more complex systems and other phases as side products which reduce the performance of the coating. Synthesizing VO_2 nanoparticles via a top-down approach using wet bead milling, we obtained particles with a switching enthalpy of

28 J/g and an amorphous fraction between 30–40% [33]. Therefore, more than one-third of the nanoparticles are non-switching VO_2. This will lead to a decrease in both the T_{vis} and ΔT_{sol}. Using a bottom-up hydrothermal approach to synthesize VO_2(M) nanoparticles, a switching enthalpy of 31 J/g with VO_2(A) as a side fraction was obtained [33]. In top-down synthesis, the purity of the VO_2(M) content can be improved via the synthesis of the VO_2 powder via calcination. Furthermore, the bead milling can be further improved to reduce the loss in crystallinity that occurs during size reduction. Here, every percentage improvement in the purity of VO_2(M) content within the nanoparticles will lead to improved thermochromic performance in the final coating.

3.3.2. Size and Distribution of Active Domains within the Matrix (Including Layer Thickness)

Particle size plays a key role in improving the optical properties of VO_2 films and coatings. To avoid Mie scattering the particles are required to be smaller than 100 nm [34]. With bead milling experiments we have increased both the T_{vis} and ΔT_{sol} by decreasing the particle size below 120 ± 10 nm [33]. Furthermore, the distribution of nanoparticles or active domains within the matrix of the coating or films is important to achieve an additional localized surface plasmon resonance (LSPR) in the metallic state of VO_2, which leads to a pronounced minimum at $\lambda \approx 1200$ nm in the transmission spectrum [30,35]. Simulation work from Zhu et al. [30] illustrates the pronounced transmission minimum when 40 nm sized VO_2 particles are homogeneously dispersed in a coating matrix, whereas agglomeration leads to the disappearance of the LSPR absorption peak and optical properties that can be associated with a continuous VO_2 layer. Due to the high solar IR intensity between 780–1360 nm, the additional absorption associated with the LSPR leads to a significant increase in ΔT_{sol}.

VO_2 content within a film or coating as well as layer thickness also play a crucial role in optimization of thermochromic properties. We have shown that changing the ratio between VO_2 and SiO_2 in a VO_2:SiO_2 composite coating at similar thickness, leads to an increased T_{vis} with reduced VO_2 content, whilst retaining a similar ΔT_{sol} [15]. Here the increased T_{vis} was associated with a change in vanadium rich domain size and morphology in TEM/EDX analysis, as well as with a lower overall VO_2 content per surface area. Surprisingly, this lower VO_2 content per surface area did not result in a significant reduction in ΔT_{sol}, which indicates that the VO_2 domain size and morphology have a significant impact on the thermochromic performance, even though the dispersion in these coatings was not good enough to result in the occurrence of an LSPR. Furthermore, we showed that by increasing the layer thickness at a constant VO_2:SiO_2 ratio, the ΔT_{sol} could be increased significantly without leading to a major reduction in T_{vis}. This was already predicted by Schläfer et al. in a previous theoretical study on VO_2:SiO_2 composite coatings [36].

3.3.3. Integration into Antireflective Coating Stack

A common strategy within the literature to improve the thermochromic performance of VO_2 coatings is to integrate a continuous VO_2 layer into a multi-layer antireflective coating stack [12]. VO_2 coatings in their monoclinic phase have a refractive index around 2.5, which leads to light reflection at the interfaces around 10% over the whole solar wavelength region between 300–2500 nm. In addition, the refractive index of rutile VO_2 after phase transition is reduced to around 2 [37]. This leads, especially in the visible, to lower reflection and in continuous VO_2 coatings to a higher visible transmission in the hot state than in the cold state [38]. Since solar intensity per wavelength is much higher in the visible than in the IR, such an increase in T_{vis} upon switching leads to a significant reduction in ΔT_{sol}. By integrating a VO_2 layer into an anti-reflective coating stack, the refractive indices and thicknesses of the individual layers within the stack can be matched to significantly increase the transmission in the monoclinic state. Since only exact matching leads to destructive interference and reduced reflection, the same effect does not occur when the refractive index of the VO_2 layer changes upon switching. Therefore, the transmission

in the hot state remains low, whilst the transmission in the cold state is increased. This simultaneously increases T_{vis} and ΔT_{sol} and can lead to high solar modulations of up to 21.8% [28]. Even though in a composite coating, the refractive index of the layer is already adjusted via the coating matrix to get rid of the effect of increasing T_{vis} upon switch, a further reduction in reflection via integration into an anti-reflective coating stack can also improve the thermochromic properties.

3.3.4. Other Strategies

Recently, more advanced strategies to improve the thermochromic performance of VO_2 coatings have been reported. Here a strategy is to combine VO_2 with another thermochromic material that changes transmission in the visible [39]. This way the overall solar modulation can be improved significantly. However, with tinting in the visible an additional effect is added to the coating, which changes the application area and is therefore not directly comparable.

Another strategy is to take advantage of the changing solar angle of incidence in summer and winter. Here, periodically patterned VO_2 coatings are prepared that enable transmission of sunlight at low angles of incidence without blocking by the VO_2 layer, whereas at higher angles of incidence, the light hits the patterned surface at the VO_2 domains and is therefore blocked [40]. Theoretically very high ΔT_{sol}. values of up to 25.8% can be achieved with this strategy. However, the concept still has to be validated in real-life experiments.

Furthermore, optimization of thermochromic properties within an IGU can be achieved by focusing on optimizing the optical properties of the low-e coating. In this study, we have already selected the most suitable commercially available low-e coating to be combined with a thermochromic coated glass. However, still, a significant reduction in solar modulation is observed due to the IR-blocking properties of the low-e coating. To further improve the thermochromic properties of the complete IGU, it is also possible to further increase the transmission of the low-e coating. Here it is crucial to retain the low emissivity properties, to not reduce the insulation value of the glazing whilst increasing the thermochromic performance.

4. Conclusions

In conclusion, we have investigated the theoretical maximum performance of thermochromic VO_2 coatings within a state-of-the-art IGU in detail. We have demonstrated that by focusing on the IR region of sunlight alone, the potential modulation range is limited to 39.1% for a single clear glass pane. We have shown that this range is further reduced by the low-e coated glass in HR++ glazing, which is necessary to reach the market standard insulation properties of IGUs. A careful selection of the most suitable low-e coating can limit this reduction and still enables a potential solar modulation of 19%, which can be increased to 23.1% when a small modulation of 10% in the visible is allowed. Larger modulation of visible light is not desired since the appearance of the IGU should remain (nearly) unchanged. In addition, we have demonstrated that our current best-performing VO_2 coating shows a solar modulation of 13.4% in combination with a low-e coated glass within an IGU. This represents a performance of 59% of the theoretical maximum. Lastly, we have discussed various strategies to further improve the thermochromic performance of such an IGU to proceed toward the theoretical maximum performance. Here especially increasing the purity of active material, and optimizing active domain size, size distribution, and layer thickness seem to be the best strategies to reach this goal.

Supplementary Materials: The following supporting information can be downloaded at: https://www.mdpi.com/article/10.3390/en16134984/s1, Figure S1: Built up of IGU; Figure S2: AM1.5 solar spectrum.

Author Contributions: D.M.: conceptualization, methodology, validation, writing—original draft, writing—review & editing, visualization; L.C.: investigation, validation, writing—original draft, writing—review & editing; C.P.K.Y.: validation, formal analysis, visualization; R.H.: validation;

K.E.: conceptualization, reviewing; A.H.: supervision, resources, reviewing; M.K.V.B.: supervision, funding acquisition, reviewing; P.B.: conceptualization, writing—review & editing, supervision. All authors have read and agreed to the published version of the manuscript.

Funding: The research work in this paper was carried out within Brightlands Materials Center, a joint research initiative between TNO and the province of Limburg. The work is funded by the Dutch government as well as the province of Limburg. Additionally, the work was partly performed within the Interreg Vlaanderen-Nederland project Sunovate and the OP Zuid project LEEF.

Conflicts of Interest: The authors declare that they have no known competing financial interests or personal relationships that could have appeared to influence the work reported in this paper.

References

1. Aditya, L.; Mahlia, T.M.I.; Rismanchi, B.; Ng, H.M.; Hasan, M.H.; Metselaar, H.S.C.; Muraza, O.; Aditiya, H.B. A review on insulation materials for energy conservation in buildings. *Renew. Sustain. Energy Rev.* **2017**, *73*, 1352–1365. [CrossRef]
2. Beute, F.; de Kort, Y.A.W. Salutogenic Effects of the Environment: Review of Health Protective Effects of Nature and Daylight. *Appl. Psychol. Health Well-Being* **2014**, *6*, 67–95. [CrossRef]
3. Mann, D.; Yeung, C.; Habets, R.; Vroon, Z.; Buskens, P. Comparative Building Energy Simulation Study of Static and Thermochromically Adaptive Energy-Efficient Glazing in Various Climate Regions. *Energies* **2020**, *13*, 2842. [CrossRef]
4. Tsikaloudaki, K.; Theodosiou, T.; Laskos, K.; Bikas, D. Assessing cooling energy performance of windows for residential buildings in the Mediterranean zone. *Energy Convers. Manag.* **2012**, *64*, 335–343. [CrossRef]
5. Jaber, S.; Ajib, S. Thermal and economic windows design for different climate zones. *Energy Build.* **2011**, *43*, 3208–3215. [CrossRef]
6. Solar Control. Available online: https://www.pilkington.com/en-gb/uk/products/product-categories/solar-control (accessed on 30 November 2022).
7. Kirimtat, A.; Koyunbaba, B.K.; Chatzikonstantinou, I.; Sariyildiz, S. Review of simulation modeling for shading devices in buildings. *Renew. Sustain. Energy Rev.* **2016**, *53*, 23–49. [CrossRef]
8. Ke, Y.; Chen, J.; Lin, G.; Wang, S.; Zhou, Y.; Yin, J.; Lee, P.S.; Long, Y. Smart Windows: Electro-, Thermo-, Mechano-, Photochromics, and Beyond. *Adv. Energy Mater.* **2019**, *9*, 1902066. [CrossRef]
9. SageGlass. Available online: https://www.sageglass.com/ (accessed on 30 November 2022).
10. HALIO. Available online: https://halioinc.com/ (accessed on 30 November 2022).
11. Granqvist, C.G.; Arvizu, M.A.; Bayrak Pehlivan, I.; Qu, H.-Y.; Wen, R.-T.; Niklasson, G.A. Electrochromic materials and devices for energy efficiency and human comfort in buildings: A critical review. *Electrochim. Acta* **2018**, *259*, 1170–1182. [CrossRef]
12. Cui, Y.; Ke, Y.; Liu, C.; Chen, Z.; Wang, N.; Zhang, L.; Zhou, Y.; Wang, S.; Gao, Y.; Long, Y. Thermochromic VO_2 for energy-efficient smart windows. *Joule* **2018**, *2*, 1707–1746. [CrossRef]
13. Zhang, Z.; Zhang, L.; Zhou, Y.; Cui, Y.; Chen, Z.; Liu, Y.; Li, J.; Long, Y.; Gao, Y. Thermochromic Energy Efficient Windows: Fundamentals, Recent Advances, and Perspectives. *Chem. Rev.* **2023**, *123*, 7025–7080. [CrossRef]
14. Chang, T.-C.; Cao, X.; Bao, S.-H.; Ji, S.-D.; Luo, H.-J.; Jin, P. Review on thermochromic vanadium dioxide based smart coatings: From lab to commercial application. *Adv. Manuf.* **2018**, *6*, 1–19. [CrossRef]
15. Yeung, C.P.K.; Habets, R.; Leufkens, L.; Colberts, F.; Vroon, Z.; Mann, D.; Buskens, P. Phase separation of VO_2 and SiO_2 on SiO_2-Coated float glass yields robust thermochromic coating with unrivalled optical properties. *Sol. Energy Mater. Sol. Cells* **2021**, *230*, 111256. [CrossRef]
16. Mann, D.; Yeung, C.P.K.; Habets, R.; Van Zandvoort, R.; Leufkens, L.; Hupperetz, J.; Out, D.; Valckenborg, R.; Vroon, Z.; Buskens, P. SunSmart—The First Affordable, Energy Optimized Smart Window. *IOP Conf. Ser. Earth Environ. Sci.* **2022**, *1085*, 012060. [CrossRef]
17. Chang, Q.; Wang, D.; Zhao, Z.; Ling, C.; Wang, C.; Jin, H.; Li, J. Size-Controllable M-Phase VO_2 Nanocrystals for Flexible Thermochromic Energy-Saving Windows. *ACS Appl. Nano Mater.* **2021**, *4*, 6778–6785. [CrossRef]
18. Okada, M.; Kuno, M.; Yamada, Y. Fast synthesis of monoclinic VO_2 nanoparticles by microwave-assisted hydrothermal method and application to high-performance thermochromic film. *Sol. Energy Mater. Sol. Cells* **2023**, *255*, 112311. [CrossRef]
19. Calvi, L.; Leufkens, L.; Yeung, C.P.K.; Habets, R.; Mann, D.; Elen, K.; Hardy, A.; Van Bael, M.K.; Buskens, P. A Comparative Study on the Switching Kinetics of W/VO_2 Powders and VO_2 Coatings and Their Implications for Thermochromic Glazing. *Sol. Energy Mater. Sol. Cells* **2021**, *224*, 110977. [CrossRef]
20. Calvi, L.; van Zandvoort, R.; Leufkens, L.; Hupperetz, J.F.B.; Habets, R.; Mann, D.; Meulendijks, N.; Elen, K.; Verheijen, M.A.; Hardy, A.; et al. Thermochromic glass laminates comprising W/VO_2 nanoparticles obtained by wet bead milling: An in-depth study of the switching performance. *Sol. Energy Mater. Sol. Cells* **2023**, *257*, 112350. [CrossRef]
21. Kim, Y.; Yu, S.; Park, J.; Yoon, D.; Dayaghi, A.M.; Kim, K.J.; Ahn, J.S.; Son, J. High-throughput roll-to-roll fabrication of flexible thermochromic coatings for smart windows with VO_2 nanoparticles. *J. Mater. Chem. C* **2018**, *6*, 3451–3458. [CrossRef]
22. Mann, D.; Yeung, C.P.K.; Habets, R.; Vroon, Z.; Buskens, P. Building energy simulations for different building types equipped with a high performance thermochromic smart window. *IOP Conf. Ser. Earth Environ. Sci.* **2021**, *855*, 012001. [CrossRef]
23. Warwick, M.E.A.; Ridley, I.; Binions, R. The effect of variation in the transition hysteresis width and gradient in thermochromic glazing systems. *Sol. Energy Mater. Sol. Cells* **2015**, *140*, 253–265. [CrossRef]

24. Hutchins, M.G.; Platzer, W.J. The thermal performance of advanced glazing materials. *Renew. Energy* **1996**, *8*, 540–545. [CrossRef]
25. Cao, X.; Chang, T.; Shao, Z.; Xu, F.; Luo, H.; Jin, P. Challenges and Opportunities toward Real Application of VO2-Based Smart Glazing. *Matter* **2020**, *2*, 862–881. [CrossRef]
26. *EN 410*; Glass in Building-Determination of Luminous and Solar Characteristics of Glazing. Comite Europeen de Normalisation: Brussels, Belgium, 2011.
27. International Glazing Database (IGDB). WINDOW Software and Optics Software, Lawrence Berkley National Laboratory, University of California. Available online: https://windows.lbl.gov/software (accessed on 30 November 2022).
28. Sol, C.; Portnoi, M.; Li, T.; Gurunatha, K.L.; Schläfer, J.; Guldin, S.; Parkin, I.P.; Papakonstantinou, I. High-Performance Planar Thin Film Thermochromic Window via Dynamic Optical Impedance Matching. *ACS Appl. Mater. Interfaces* **2020**, *12*, 8140–8145. [CrossRef]
29. Zhou, Y.; Huang, A.; Li, Y.; Ji, S.; Gao, Y.; Jin, P. Surface plasmon resonance induced excellent solar control for VO_2@SiO_2 nanorods-based thermochromic foils. *Nanoscale* **2013**, *5*, 9208–9213. [CrossRef]
30. Zhu, J.; Zhou, Y.; Wang, B.; Zheng, J.; Ji, S.; Yao, H.; Luo, H.; Jin, P. Vanadium Dioxide Nanoparticle-based Thermochromic Smart Coating: High Luminous Transmittance, Excellent Solar Regulation Efficiency and Near Room Temperature Phase Transition. *ACS Appl. Mater. Interfaces* **2015**, *7*, 27796–27803. [CrossRef]
31. Srivastava, A.; Rotella, H.; Saha, S.; Pal, B.; Kalon, G.; Mathew, S.; Motapothula, M.; Dykas, M.; Yang, P.; Okunishi, E.; et al. Selective growth of single phase VO_2 (A, B, and M) polymorph thin films. *APL Mater.* **2015**, *3*, 026101. [CrossRef]
32. Kniec, K.; Marciniak, L. Different Strategies of Stabilization of Vanadium Oxidation States in $Lagao_3$ Nanocrystals. *Front. Chem.* **2019**, *7*, 520. [CrossRef]
33. Calvi, L.; van Geijn, R.; Leufkens, L.; Habets, R.; Gurunatha, K.L.; Stout, K.; Mann, D.; Papakonstantinou, I.; Parkin, I.P.; Elen, K.; et al. The Impact of Bead Milling on the Thermodynamics and Kinetics of the Structural Phase Transition of VO_2 Particulate Materials and Their Potential for Use in Thermochromic Glazing. *Sol. Energy Mater. Sol. Cells* **2022**, *242*, 111783. [CrossRef]
34. Lockwood, D.J. Rayleigh and Mie Scattering. In *Encyclopedia of Color Science and Technology*; Luo, M.R., Ed.; Springer: New York, NY, USA, 2016.
35. Wang, D.; Guo, D.; Zhao, Z.; Ling, C.; Li, J.; Hong, S.; Zhao, Y.; Jin, H. Surface modification-assisted solvent annealing to prepare high quality M-phase VO_2 nanocrystals for flexible thermochromic films. *Sol. Energy Mater. Sol. Cells* **2019**, *200*, 110031. [CrossRef]
36. Schläfer, J.; Sol, C.; Li, T.; Malarde, D.; Portnoi, M.; Macdonald, T.J.; Laney, S.K.; Powell, M.J.; Top, I.; Parkin, I.P.; et al. Thermochromic VO_2–SiO_2 nanocomposite smart window coatings with narrow phase transition hysteresis and transition gradient width. *Sol. Energy Mater. Sol. Cells* **2019**, *200*, 109944. [CrossRef]
37. Currie, M.; Mastro, M.A.; Wheeler, V.D. Characterizing the tunable refractive index of vanadium dioxide. *Opt. Mater. Express* **2017**, *7*, 1697–1707. [CrossRef]
38. Mlyuka, N.R.; Niklasson, G.A.; Granqvist, C.G. Mg doping of thermochromic VO_2 films enhances the optical transmittance and decreases the metal-insulator transition temperature. *Appl. Phys. Lett.* **2009**, *95*, 171909. [CrossRef]
39. Zhu, J.; Huang, A.; Ma, H.; Tong, K.; Ji, S.; Bao, S.; Cao, X.; Jin, P. Composite Film of Vanadium Dioxide Nanoparticles and Ionic Liquid-nickel-chlorine Complexes with Excellent Visible Thermochromic Performance. *ACS Appl. Mater. Interfaces* **2016**, *8*, 29742–29748. [CrossRef]
40. Zhou, C.; Li, D.; Tan, Y.; Ke, Y.; Wang, S.; Zhou, Y.; Liu, G.; Wu, S.; Peng, J.; Li, A.; et al. 3D Printed Smart Windows for Adaptive Solar Modulations. *Adv. Opt. Mater.* **2020**, *8*, 2000013. [CrossRef]